Differentiation of Murine Colon Pathology by Optical and Mechanical Contrast using Optical Coherence Tomography and Elastography

Achuth Nair[1], Susobhan Das[1], Chih-Hao Liu[1], Manmohan Singh[1], Triet Le[1], Salavat Aglyamov[2,3], Yong Du[1], Sanam Soomro[1], Chandra Mohan[1], and Kirill V. Larin[1,4,5,*]

[1]Department of Biomedical Engineering, University of Houston, Houston, TX, USA
[2]Department of Mechanical Engineering, University of Houston, Houston, TX, USA
[3]Department of Biomedical Engineering, University of Texas at Austin, Austin, TX, USA
[4]Interdisciplinary Laboratory of Biophotonics, Tomsk State University, Tomsk, Russia
[5]Molecular Physiology and Biophysics, Baylor College of Medicine, Houston, TX, USA
*klarin@uh.edu

ABSTRACT

Colon pathologies including colon cancer and ulcerative colitis afflict hundreds of thousands of people in the United States. Clinical detection of colon diseases is generally performed through colonoscopy. However, these methods usually lack the sensitivity or resolution to detect diseased tissue at early stages. Even high resolution optical techniques such as confocal microscopy and optical coherence tomography (OCT) rely on structural features to detect anomalies in tissue, which may not be sufficient for early disease detection. If changes in tissue biomechanical properties precede morphological changes in tissue physiology, then mechanical contrast would enable earlier detection of disease. In this work, we utilized optical coherence elastography (OCE) to assess the biomechanical properties of healthy, cancerous, and colitis tissue. Additionally, the optical properties of each sample were also assessed as a secondary feature to distinguish tissue types. The Young's modulus, as measured by the propagation of an elastic wave, of the healthy, cancerous, and colitis tissue was 10.8 ± 1.0 kPa, 7.12 ± 1.0 kPa, and 5.1 ± 0.1 kPa, respectively. The variations in the OCT signal intensity over depth, as measured by the slope-removed standard deviation of each A-scan was 5.8 ±.0.3 dB, 5.1 ± 0.4 dB, and 5.5 ± 0.2 dB for healthy, cancerous, and colitis tissue, respectively. This work shows OCT structural imaging combined with OCE can detect minute changes in colon tissue optical scattering and elastic properties, which may be useful for detection various colon diseases, such as colitis and colon cancer.

Keywords: inflammatory bowel disease, ulcerative colitis, colorectal cancer, Young's Modulus, elastography, optical coherence tomography

1. INTRODUCTION

Colorectal pathologies afflict millions of people worldwide. The global burden of colorectal cancer (CRC) is fourth leading cause of cancer death in the world, with as much as 60% of CRC related deaths occurring in highly developed countries [1]. Similarly, the prevalence of Inflammatory bowel diseases (IBD) such as ulcerative colitis (UC) has risen to more than 0.3% of the population of North America, Australia, and several European countries [2]. Furthermore, past meta analyses have shown a colorectal cancer prevalence of 3.7% in patients that have ulcerative colitis [2]. Colorectal pathologies may have a high burden of illness since they can be related to high morbidity and decreased quality of life [3]. As such, diagnostic tools are critical for early detection and treatment of these conditions. The primary clinical tool for studying colorectal pathologies is colonoscopy [4]. However, it has limited spatial resolution, cannot provide depth-wise information, and can only perform structural imaging. Ultrasonic techniques have been proposed for depth-resolved colorectal imaging and subsequent pathology detection, but still have limited spatial resolution [5, 6]. Optical techniques show great promise for detection of colorectal lesions with

Optical Elastography and Tissue Biomechanics VI, edited by Kirill V. Larin, Giuliano Scarcelli, Proc. of SPIE
Vol. 10880, 108800P · © 2019 SPIE · CCC code: 1605-7422/19/$18 · doi: 10.1117/12.2510183

high resolution and depth resolved imaging [7-9]. However, structural imaging modalities are limited without a quantifiable metric for differentiating diseased and healthy tissue.

Elastography is a method of imaging mechanical contrast in tissue utilizing imaging modalities, such as ultrasound and magnetic resonance imaging [10, 11]. Magnetic resonance elastography and ultrasound elastography have been used to distinguish gastroenterological pathologies including ulcerative colitis and colorectal cancer, but both methods are limited by the spatial resolution of their parent imaging modality and require large amplitude displacements for accurate detection, which may not be suitable to detect small lesions [12, 13]. Ultrasound elastography has been utilized to assess the relative strain of cancerous colorectal adenoma, but to our knowledge, absolute measurements of mechanical properties have not been shown [5, 14].

Optical coherence elastography (OCE) is an emerging technique that utilizes the noninvasive nature and high spatial resolution of OCT to obtain micrometer-scale resolution and sub-nanometer scale displacement sensitivity with phase-resolved detection [15-17]. OCE has the potential to detect microscopic lesions due to its superior resolution and sensitivity. OCE has been used to detect soft tissue tumors, assess cancer margins, and to evaluate the elasticity of thin tissues such as the cornea [16, 18, 19]. Moreover, probe-based OCE has been demonstrated with potential uses in endoscopic applications, but to our knowledge, OCE in gastroenterology has been limited [7].

In this work, we performed noncontact air pulse OCE measurements on *ex-vivo* healthy, ulcerative, and cancerous murine colon tissue [20]. Measurements were taken at six positions along the tissue and averaged to obtain a regional measurements of sample elasticity based on the velocity of an air-pulse induced elastic wave. Tissue optical properties were evaluated by analyzing the OCT signal at each measured position. These measurements were then used to distinguish healthy and diseased tissue based on optical and elastic properties.

2. MATERIALS AND METHODS

OCE measurements were performed on sixteen extracted murine colon specimens. Imaging and analysis were performed blindly on each sample such that disease or healthy condition was not known prior to extracting experimental results to ensure unbiased testing. Diseased samples were symptomatic of UC or CRC induced by dextran sulfate sodium (DSS). Each colon sample was placed on a 1% nutrient agar phantom base and was spread out carefully to expose the maximum testing region without structurally compromising the tissue. Each sample was regularly hydrated throughout the testing period using 1X PBS. Along each sample, OCE measurements were taken at six positions.

The air pulse OCE system consisted of a phase-stabilized swept source optical coherence tomography (PhS-SSOCT) system and a synchronized air pulse device. The system setup shown in Figure 1 is well described in our previous works [21-23]. A short duration (< 1 ms) focused micro air-pulse induced a low-amplitude (≤ 10 μm) displacement that propagated as an elastic wave on the sample surface [24]. The elastic wave was detected with 251 M-mode scans along its propagation path over a 3 mm region. Wave velocity was determined by linearly fitting the propagation distance to its corresponding temporal delay from its excitation position [25]. Velocities at each position were averaged depth-wise from the surface to 0.2 mm below the surface, which corresponds to the mucosal layer of the colon. Since the measured elasticity of the tissue would be greatly affected by boundary conditions, the elasticity of the agar basement was monitored throughout the experimental procedure to identify degradation of the basement. Wave velocities were translated to Young's modulus using the surface wave equation (SuWE) [26].

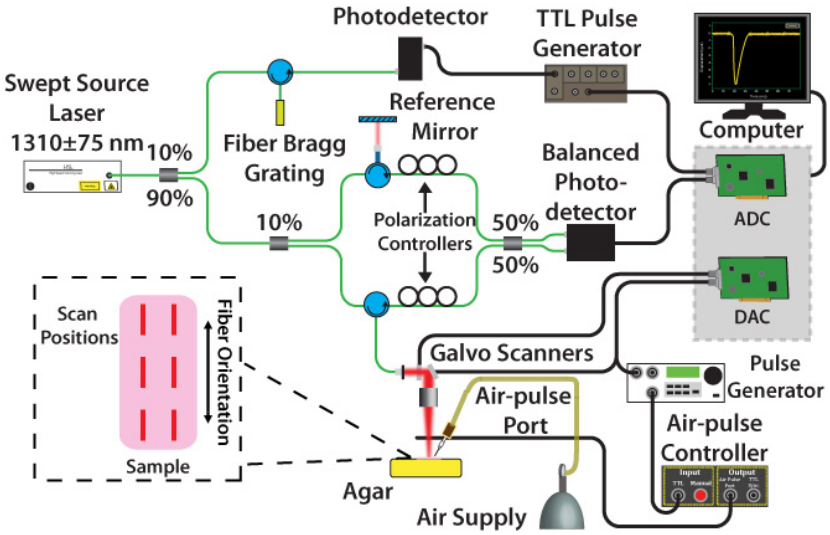

Figure 1: Schematic of the experimental setup.

Optical analysis of the tissue was performed by analyzing each A-scan in log scale from the OCT structural image obtained during OCE imaging. Due to the refractive index change at the air-sample interface, high reflections usually occur at the sample surface. To remove the influence of this region on computation, the computational window began ~40 μm below the sample surface. The A-scan was linearly fitted, and the slope was subtracted from the A-scan. The standard deviation of the slope-removed A-scan was calculated and represents the axial refractive index mismatches throughout the calculation window [27, 28]. The values were then average for each imaged region.

Sample elasticity and standard deviation of the intensity signal at all positions were averaged for each sample. One sample in the ulcerative colitis group was removed due to degradation of the basement layer, which significantly affected the OCE measurement. The diseased state, which was determined prior to OCE imaging, was revealed after the OCE measurements, and the results were grouped accordingly for statistical analysis.

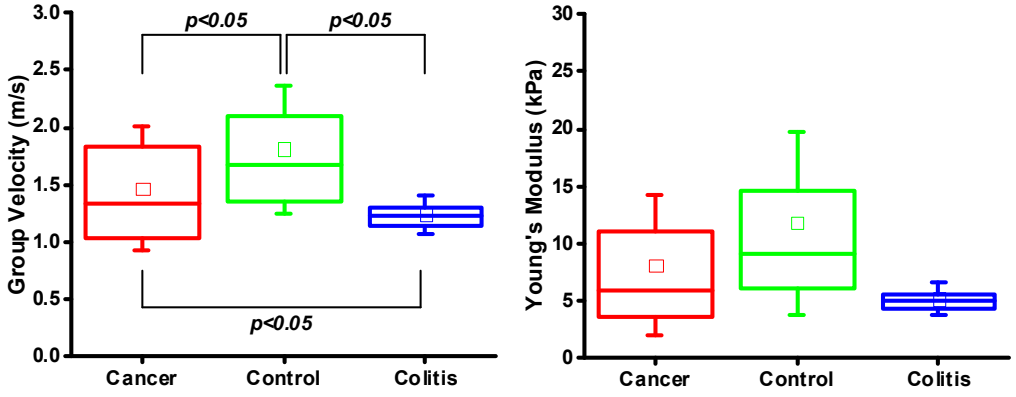

Figure 2: Group velocity and Young's modulus of each murine sample group (N=4 cancer, N=4 colitis, and N=8 control). Box and whiskers show the IQR and 1 standard deviation respectively. Statistical testing was performed using a two-sample unequal variances t-test for the measured parameter— group velocity.

3. RESULTS

Figure 1 shows the group velocity and Young's modulus obtained using the SuWE for each sample group, in which there are four cancerous, eight control, and four colitis samples respectively. The group velocity for the cancer, control and colitis tissues are 1.5 ± 0.5 m/s, 1.8 ± 0.6 m/s, and 1.2 ± 0.2 m/s, respectively. The Young's modulus for the cancer, control, and colitis tissues are 7.12 ± 1.0 kPa, 10.8 ± 1.0 kPa, and 5.1 ± 0.1 kPa, respectively. A two-sample unequal variances t-test of group velocity, the measured parameter, showed a statistically significant difference between each group. The cancerous and colitis samples were significantly less stiff than the samples in the control group.

Figure 2 presents the analysis of the optical properties for each sample group, showing the average slope-removed standard deviation of the intensity signal. For each sample group, standard deviations were computed as 5.1 ± 0.4 dB, 5.8 ±.0.3 dB, and 5.5 ± 0.2 dB for cancer, control, and colitis murine colon respectively. The high standard deviation in the control group compared to diseased tissue indicates a greater degree refractive index mismatching, which corresponds to tissue structural heterogeneity.

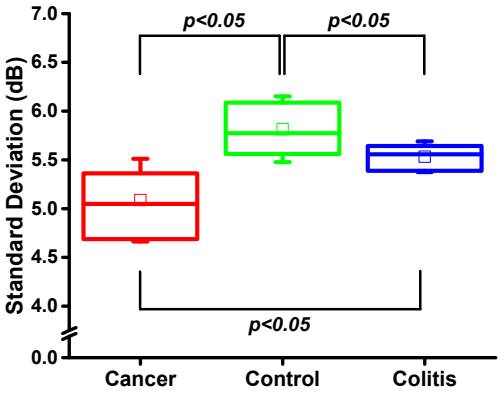

Figure 3: Standard deviation of the slope removed A-line for each sample group, representing the refractive index mismatch within each sample, with N=4 cancer, N=4 colitis, and N=8 control. Box and whisker show the IQR and 1 standard deviation respectively. Statistical testing was performed with a two-sample unequal variances t-test.

Our r urine colon tissue. Group velocity analysis shows a statistically significant difference in stiffness between each tissue type, though there are limitations with this calculation procedure. For example, since each sample was placed on an agar basement layer, boundary conditions may affect the absolute measurement of tissue elasticity. Additionally, sample geometry, including thickness, can also affect the velocity of the elastic wave [26]. Analysis of the dispersive behavior of the elastic wave may address concerns with sample geometry and boundary conditions, particularly with robust analytical wave models [29]. We are currently developing a multi-layer wave model that can correctly integrate the sample geometry and measurement conditions to provide quantitative, and potentially depth-resolved, biomechanical assessments of tissues. Additionally, we are exploring alternative excitation techniques with higher frequency content, which would increase spatial resolution and reduce influence of boundary conditions. Furthermore, quasi-static OCE techniques such as compression OCE show great promise in assessing mechanical contrast of tissue with high spatial resolution [16].

Optical analysis of the murine tissue showed distinct differences between each group. The standard deviation of the slope-removed intensity signal reflects the refractive index mismatch in the sample through depth, which is indicative of the sample morphological heterogeneity. Further investigation with histopathology is needed to corroborate these results.

5. CONCLUSION

In this work, OCE was used to differentiate the elastic properties of healthy, cancerous and colitis *ex vivo* murine colon tissue. The results show that healthy tissue appeared to be stiffer than the diseased tissue based on OCE measurement of surface wave velocity. However, further study into the dispersive properties of the elastic wave are needed to verify the results and integrate sample geometry and boundary conditions that may affect the measured results. Additionally, the optical properties of the tissue were evaluated. The standard deviation of the slope-removed OCT intensity signal indicated a significantly higher degree of refractive index mismatches over depth in the healthy tissue in comparison to the diseased tissue. Our results show that OCE could be useful for early detection of colon tissue pathologies.

ACKNOWLEDGEMENTS

This work was supported, in part, by: the U.S. National Institutes of Health (NIH) grants 2R01EY022362, 1R01HL120140; U.S. Department of Defense (DOD) Congressionally Directed Medical Research Programs (CDMRP) grant PR150338.

REFERENCES

[1] M. Arnold, M. S. Sierra, M. Laversanne *et al.*, "Global patterns and trends in colorectal cancer incidence and mortality," Gut, 66(4), 683-691 (2017).

[2] J. A. Eaden, K. R. Abrams, and J. F. Mayberry, "The risk of colorectal cancer in ulcerative colitis: a meta-analysis," Gut, 48(4), 526 (2001).

[3] M. D. Kappelman, S. L. Rifas-Shiman, K. Kleinman *et al.*, "The prevalence and geographic distribution of Crohn's disease and ulcerative colitis in the United States," Clin Gastroenterol Hepatol, 5(12), 1424-9 (2007).

[4] R. Rameshshanker, and N. Arebi, "Endoscopy in inflammatory bowel disease when and why," World J Gastrointest Endosc, 4(6), 201-11 (2012).

[5] J. Panes, R. Bouzas, M. Chaparro *et al.*, "Systematic review: the use of ultrasonography, computed tomography and magnetic resonance imaging for the diagnosis, assessment of activity and abdominal complications of Crohn's disease," Aliment Pharmacol Ther, 34(2), 125-45 (2011).

[6] M. Ellrichmann, P. Wietzke-Braun, S. Dhar *et al.*, "Endoscopic ultrasound of the colon for the differentiation of Crohn's disease and ulcerative colitis in comparison with healthy controls," Aliment Pharmacol Ther, 39(8), 823-33 (2014).

[7] T.-H. Tsai, C. L. Leggett, A. J. Trindade *et al.*, "Optical coherence tomography in gastroenterology: a review and future outlook." 22, 17.

[8] A. Dhar, K. S. Johnson, M. R. Novelli *et al.*, "Elastic scattering spectroscopy for the diagnosis of colonic lesions: initial results of a novel optical biopsy technique," Gastrointest Endosc, 63(2), 257-61 (2006).

[9] O. Watanabe, T. Ando, O. Maeda *et al.*, "Confocal endomicroscopy in patients with ulcerative colitis," J Gastroenterol Hepatol, 23 Suppl 2, S286-90 (2008).

[10] Y. Li, and J. G. Snedeker, "Elastography: modality-specific approaches, clinical applications, and research horizons," Skeletal Radiol, 40(4), 389-97 (2011).

[11] K. J. Parker, M. M. Doyley, and D. J. Rubens, "Imaging the elastic properties of tissue: the 20 year perspective," Phys Med Biol, 56(1), R1-R29 (2011).

[12] L. Juge, B. T. Doan, J. Seguin *et al.*, "Colon tumor growth and antivascular treatment in mice: complementary assessment with MR elastography and diffusion-weighted MR imaging," Radiology, 264(2), 436-44 (2012).

[13] F. Branchi, F. Caprioli, S. Orlando *et al.*, "Non-invasive evaluation of intestinal disorders: The role of elastographic techniques," World J Gastroenterol, 23(16), 2832-2840 (2017).

[14] D. Ishikawa, T. Ando, O. Watanabe *et al.*, "Images of colonic real-time tissue sonoelastography correlate with those of colonoscopy and may predict response to therapy in patients with ulcerative colitis," BMC Gastroenterology, 11(1), 29 (2011).

[15] J. Schmitt, "OCT elastography: imaging microscopic deformation and strain of tissue," Opt Express, 3(6), 199-211 (1998).

[16] K. V. Larin, and D. D. Sampson, "Optical coherence elastography - OCT at work in tissue biomechanics [Invited]," Biomed Opt Express, 8(2), 1172-1202 (2017).

[17] S. Wang, J. Li, R. K. Manapuram *et al.*, "Noncontact measurement of elasticity for the detection of soft-tissue tumors using phase-sensitive optical coherence tomography combined with a focused air-puff system," Opt Lett, 37(24), 5184-6 (2012).

[18] S. Wang, and K. V. Larin, "Optical coherence elastography for tissue characterization: a review," J Biophotonics, 8(4), 279-302 (2015).

[19] B. F. Kennedy, K. M. Kennedy, A. L. Oldenburg *et al.*, [Optical Coherence Elastography] Springer International Publishing, Cham(2015).

[20] I. Okayasu, S. Hatakeyama, M. Yamada *et al.*, "A novel method in the induction of reliable experimental acute and chronic ulcerative colitis in mice," Gastroenterology, 98(3), 694-702 (1990).

[21] W. Shang, K. V. Larin, L. Jiasong *et al.*, "A focused air-pulse system for optical-coherence-tomography-based measurements of tissue elasticity," Laser Physics Letters, 10(7), 075605 (2013).

[22] R. K. Manapuram, S. Aglyamov, F. M. Menodiado *et al.*, "Estimation of shear wave velocity in gelatin phantoms utilizing PhS-SSOCT," Laser Physics, 22(9), 1439-1444 (2012).
[23] S. Wang, and K. V. Larin, "Shear wave imaging optical coherence tomography (SWI-OCT) for ocular tissue biomechanics," Opt Lett, 39(1), 41-4 (2014).
[24] S. Wang, K. V. Larin, J. Li *et al.*, "A focused air-pulse system for optical-coherence-tomography-based measurements of tissue elasticity," Laser Phys Lett, 10(7), 075605 (2013).
[25] S. Wang, A. L. Lopez, 3rd, Y. Morikawa *et al.*, "Noncontact quantitative biomechanical characterization of cardiac muscle using shear wave imaging optical coherence tomography," Biomed Opt Express, 5(7), 1980-92 (2014).
[26] J. F. Doyle, [Wave Propagation in Structures Spectral Analysis Using Fast Discrete Fourier Transform] New York:Springer, (1997).
[27] S. Wang, C. Liu, V. P Zakharov *et al.*, [Three-dimensional computational analysis of optical coherence tomography images for the detection of soft tissue sarcomas], (2014).
[28] C. H. Liu, Y. Du, M. Singh *et al.*, "Classifying murine glomerulonephritis using optical coherence tomography and optical coherence elastography," Journal of Biophotonics, 9(8), 781-791 (2016).
[29] L. Yung-Chun, J. O. Kim, and J. D. Achenbach, "Acoustic microscopy measurement of elastic constants and mass density," IEEE Transactions on Ultrasonics, Ferroelectrics and Frequency Control, 42(2), 253-264 (1995).